iScience

CellPress
OPEN ACCESS

Article

Lactate facilitates classical swine fever virus replication by enhancing cholesterol biosynthesis

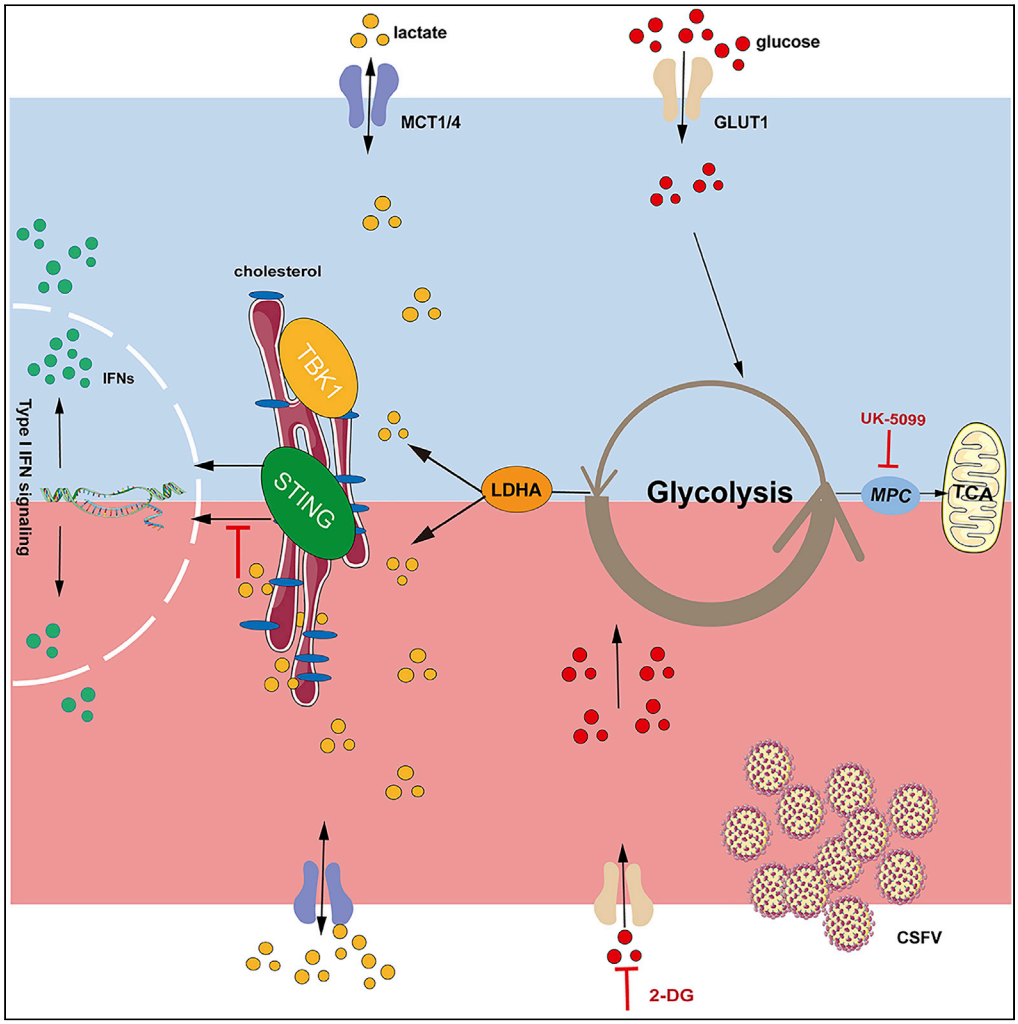

Xiaodong Zou, Yang Yang, Feng Lin, ..., Daxin Pang, Linzhu Ren, Xiaochun Tang

renlz@jlu.edu.cn (L.R.)
xiaochuntang@jlu.edu.cn (X.T.)

Highlights

Aerobic glycolysis plays an important role in CSFV replication

Intracellular lactate maintains CSFV replication as an effector of glycolysis

Lactate promotes cholesterol biosynthesis to maintain CSFV replication

Enhanced cholesterol biosynthesis inhibited the response of IFNs during CSFV replication

Zou et al., iScience 25, 105353
November 18, 2022
https://doi.org/10.1016/j.isci.2022.105353

iScience

CellPress
OPEN ACCESS

Article

Lactate facilitates classical swine fever virus replication by enhancing cholesterol biosynthesis

Xiaodong Zou,[1,3] Yang Yang,[1,3] Feng Lin,[1] Jiahuan Chen,[1] Huanyu Zhang,[1] Linquan Li,[1] Hongsheng Ouyang,[1,2] Daxin Pang,[1,2] Linzhu Ren,[1,*] and Xiaochun Tang[1,2,4,*]

SUMMARY

An emerging topic in virology is that viral replication is closely linked with the metabolic reprogramming of host cells. Understanding the effects of reprogramming host cell metabolism due to classical swine fever virus (CSFV) infection and the underling mechanisms would facilitate controlling the spread of classical swine fever (CSF). In the current study, we found that CSFV infection enhanced aerobic glycolysis in PK-15 cells. Blocking glycolysis with 2-deoxy-d-glycose or disrupting the enzymes PFKL and LDHA decreased CSFV replication. Lactate was identified as an important molecule in CSFV replication, independent of the pentose phosphate pathway and tricarboxylic acid cycle. Further analysis demonstrated that the accumulated lactate in cells promoted cholesterol biosynthesis, which facilitated CSFV replication and disrupted the type I interferon response during CSFV replication, and the disruption of cholesterol synthesis abolished the lactate effects on CSFV replication. The results provided more insights into the complex pathological mechanisms of CSFV.

INTRODUCTION

The replication and propagation of viruses in cells are dependent on host cell metabolism (Varanasi and Rouse, 2018). In recent years, we have made significant advances with respect to how viruses interact with host cell metabolism (Mayer et al., 2019). Viruses reshape host cell metabolism during infections by targeting essential metabolic regulatory proteins and generating unique metabolic states that facilitate their replication (Sumbria et al., 2020). By modulating complex signaling pathways, some viruses increase available energy and promote their reproduction by manipulating glucose metabolism (Thaker et al., 2019). It has been discovered that severe acute respiratory syndrome coronavirus 2 (SARS-CoV-2) hijacks the mitochondria of cells and manipulates the metabolic pathways of the host cell for replication (Ajaz et al., 2021). The Epstein-Barr virus (EBV) and the Zika virus enhance glucose uptake due to a reduction in AMPK phosphorylation (Lyu et al., 2018; Singh et al., 2020). The PI3K/AKT pathway is activated by the norovirus, rhinovirus, and the human immunodeficiency virus (HIV) to increase glucose transporter type 1 (GLUT1) phosphorylation and increase glycolysis flux (Gualdoni et al., 2018; Passalacqua et al., 2019; Sorbara et al., 1996).

Meanwhile, numerous reports have emphasized the effects of viral infections and replication on the important roles of host cell lipid metabolism. To gain a selective advantage and to facilitate its replication, a virus actively alters host cell lipid metabolism. For example, human cytomegalovirus and Middle East respiratory syndrome coronavirus increase SREBP1 translocation to the nuclei, and thus, increase fatty acid synthesis (Spencer et al., 2011; Yuan et al., 2019). The EBV, coxsackievirus B3, respiratory syncytial virus, and hepatitis C virus (HCV) increase the expression of fatty acid synthase and induce lipogenic gene expression (Hulse et al., 2021; Kapadia and Chisari, 2005; Ohol et al., 2015; Wilsky et al., 2012). In addition, SARS-CoV-2, HCV, Zika virus, dengue virus, West Nile virus, rotavirus, and influenza virus can alter lipid droplet (LD) compartments, trafficking, formation, or recruitment (Cheung et al., 2010; Dias et al., 2020; Episcopio et al., 2019; Hou et al., 2017; Martins et al., 2019; Samsa et al., 2009; Vogt et al., 2013).

Classical swine fever virus (CSFV) is an enclosed, single-stranded, positive-sense RNA virus, with a 12.3-kb RNA genome, which belongs to the *Pestivirus* genus of the Flaviviridae family. The genome encodes a polypeptide precursor that is cleaved by viral and cellular proteases into four structural proteins (C, Erns, E1, and E2) and eight non-structural proteins (Npro, p7, NS2, NS3, NS4A, NS4B, NS5A, and NS5B) (Ji et al., 2015).

[1]College of Animal Sciences, Jilin University, Changchun, China

[2]Chongqing Research Institute of Jilin University, Chongqing, China

[3]These authors contributed equally

[4]Lead contact

*Correspondence: renlz@jlu.edu.cn (L.R.), xiaochuntang@jlu.edu.cn (X.T.)

https://doi.org/10.1016/j.isci.2022.105353

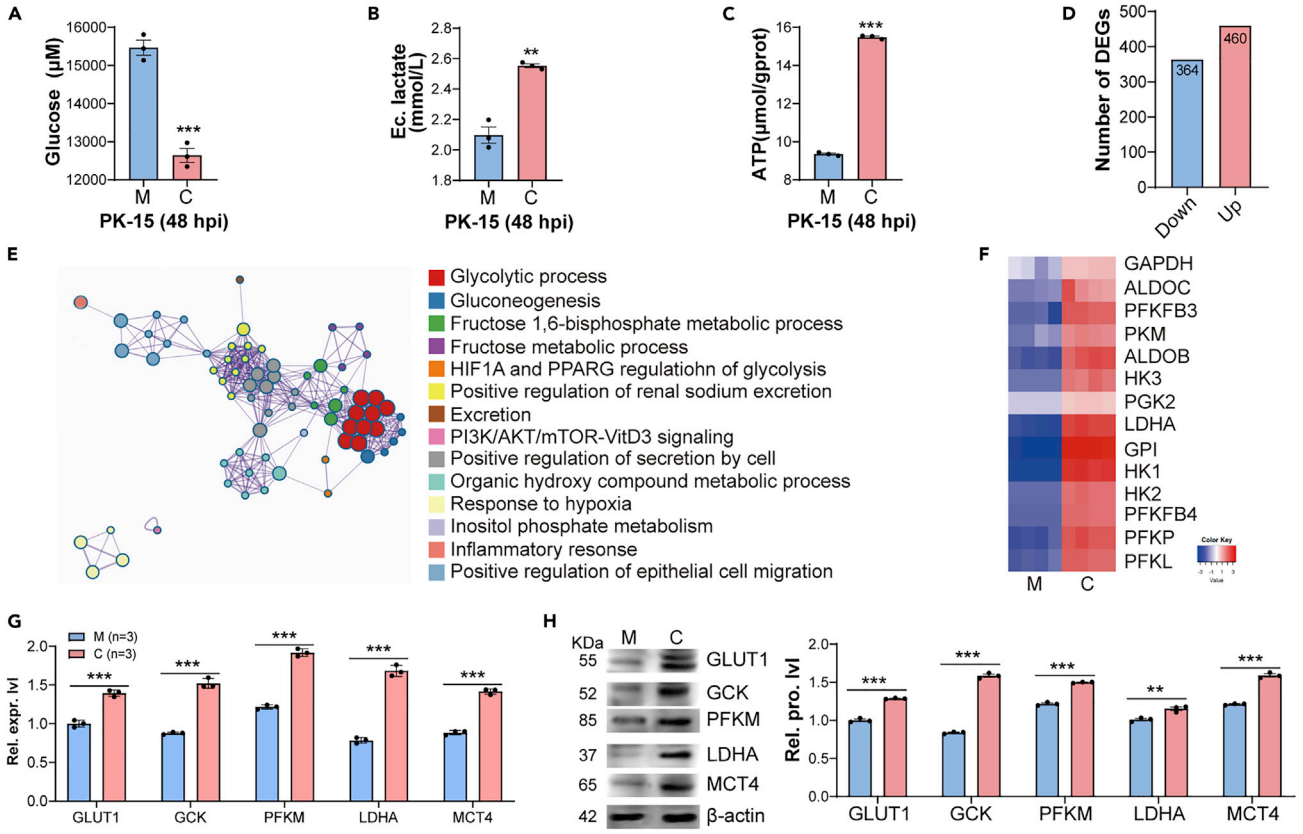

Figure 1. Aerobic glycolysis was enhanced in CSFV-infected PK-15 cells

(A–C) Measurement of glucose levels, lactate secretion, and ATP production in CSFV-infected PK-15 cells, n = 3, **p < 0.01, ***p < 0.001.

(D) In CSFV-infected PK-15 cells, a total of 824 DEGs were discovered, with 460 upregulated and 364 downregulated genes.

(E) Gene ontology (GO) enrichment for DEGs in CSFV-infected PK-15 cells.

(F) The glycolytic-related gene expression was analyzed in CSFV-infected PK-15 cells.

(G and H) The levels of transcript (G) and protein (H) expression of key glycolysis enzymes, n = 3, **p < 0.01, ***p < 0.001. (M, mock; C, CSFV; Rel. expr. lvl, relative expression level; Ec. lactate, extracellular lactate level; Rel. prot. lvl, relative protein level.)

Previous reports of proteomic analyses have indicated that CSFV infection in PK-15 cells improved the glycolytic process by increasing phosphoglycerate mutase 1 (PGAM1), glyceraldehyde-3-phosphate dehydrogenase (GAPDH), and triosephosphate isomerase (Gou et al., 2017). However, later research on the metabolic profiles in CSFV-infected PK-15 cells have shown that the glycolytic intermediates were decreased, but the lactate level was upregulated (fold change [FC] = 0.09) (Sun et al., 2008). Thus, a consensus has not been reached on the role of aerobic glycolysis in CSFV infection and replication.

Herein, we investigated the relationship between CSFV infection and aerobic glycolysis in PK-15 cells and the underlying mechanisms. The results showed that CSFV infection enhanced aerobic glycolysis and that lactate was an essential molecule in CSFV replication. In addition, lactate exerted functions by promoting cholesterol biosynthesis. The data provided more insights into the complex pathological mechanisms of CSFV.

RESULTS

CSFV enhances aerobic glycolysis in PK-15 cells

We investigated the glucose levels in a culture medium of PK-15 cells during CSFV replication. As shown in Figure 1A, a significant decrease in glucose levels was detected in the PK-15 cells during CSFV replication. Meanwhile, extracellular lactate was increased significantly when compared with that of the control group (Figure 1B). Furthermore, the ATP levels in CSFV-infected cells were elevated significantly (Figure 1C).

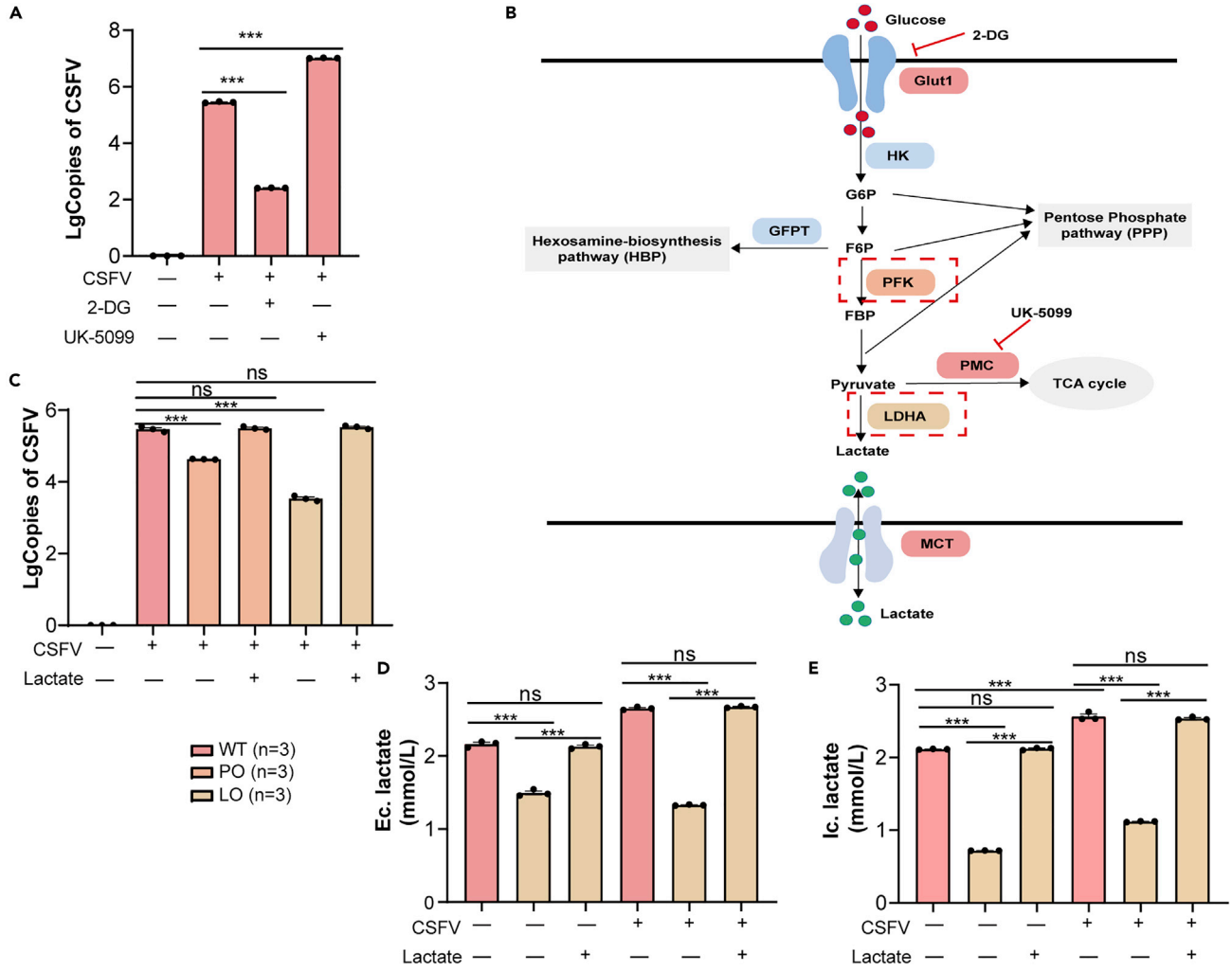

Figure 2. Aerobic glycolysis regulates CSFV replication in PK-15 cells

(A) qPCR was used to determine the number of viral genomic RNA copies present in PK-15 cells 48 h after infection, n = 3, ***p < 0.001.

(B) Diagram of the glycolytic pathway.

(C) Glycolysis disruption effectively reduced CSFV replication in PK-15 at 48 hpi, n = 3, ***p < 0.001.

(D and E) Extracellular and intracellular lactate levels in CSFV-infected PK-15 cells were measured, n = 3, ***p < 0.001. (WT, wild-type; PO, pfkl-ko; LO, ldha-ko; Ec. lactate, extracellular lactate level; Ic. lactate, intracellular lactate level.)

According to the one-step growth curve of CSFV (Figure S1A), the copy numbers of viral genomic RNAs peaked at 48 h post infection (hpi). Therefore, CSFV-infected PK-15 cells were prepared at 48 hpi for transcriptome analysis. There were 824 differentially expressed genes (DEGs) in the CSFV-infected PK-15 cells, with 460 upregulated genes and 364 downregulated genes (Figure 1D). The "glycolytic process" was discovered to be a highly enriched biological pathway (Figure 1E). In the RNA-sequencing data, transcriptional and translational expression analyses confirmed significant changes in the genes involved in glycolysis, such as the *HK2*, *PFKL*, and *LDHA* genes (Figures 1F–1H). Taken together, CSFV replication enhanced aerobic glycolysis in PK-15 cells.

Aerobic glycolysis direct involvement in CSFV replication

To investigate the effects of glycolysis on CSFV replication, the glycolytic pathway was manipulated (Figure 2B and Table 1). First, we discovered that the glucose analog 2-deoxy-d-glycose inhibited CSFV replication significantly, whereas UK-5099, a selective inhibitor of mitochondrial pyruvate carrier, enhanced the glycolysis flux and increased CSFV replication (Figure 2A). Then, to further investigate the effect of glycolysis on CSFV replication, the *PFKL* gene (PO) and the *LDHA* gene (LO) in the PK-15 cells were separately

Table 1. The primers for PCR amplification of genotyping of cell clones

Primers	Sequences (5′ to 3′)	Amplicon (bp)
PFKL-JD	GCGGTCACGTGTAAGGAACA	1164
	TTCAGAACCAGGAAGAGCCG	
LDHA-JD	CTGTCCCTGGGCTGAATGAC	974
	GCATTTCTGCGGCTATGGTG	
MCT1-JD	GCTCGGATCCTTCATTGCTG	974
	AGCAACATGGGATCTGAGGT	
SQLE-JD	GGTGTCACCGAAGAAGCCTT	819
	GAACCTCCATATGCCGCTGG	

disrupted by the CRISPR-Cas9 system. As shown in Figure 2C, CSFV replication was effectively decreased in the PO and LO cells. The disruption of the *LDHA* gene, which plays a role in the downstream of glycolysis, decreased CSFV replication more than that of the *PFKL* gene (Figure S2A). Moreover, the levels of intracellular and extracellular lactate were significantly lower in the PO and LO cells when compared with the control group. However, the addition of lactate into the culture media reversed the inhibition of CSFV replication in the LO cells (Figures 2D, 2E, and S2B–S2D). Taken together, these findings suggested that glycolysis plays an important role in CSFV replication.

Intracellular lactate maintains CSFV replication as the effector molecule of glycolysis

Previous studies have shown that many tumor and cancer cells undergo glycolysis under aerobic conditions to produce large amounts of lactate for proliferation and metastasis (Becker, 2020), and that lactate appears to be the primary cause of decreased extracellular pH in tumor tissues (Kato et al., 2013). Thus, we examined the role of extracellular lactate in CSFV replication. As shown in Figure 3A, the levels of extracellular lactate were gradually increased and extracellular pH levels were continuously decreased along with the time of CSFV replication. To identify the pH effects caused by lactate on CSFV replication, we prepared culture mediums with various pH values by using the addition of lactate. When compared with the control group, different pH values did not affect CSFV replication in the PK-15 cells (Figure 3C). Along with the CSFV replication, the level of intracellular lactate reached a peak at 48 hpi when compared with the control group (Figure 3D). To investigate the effects of intracellular lactate, we disrupted lactate monocarboxylate transporter 1 (*MCT1*), which is responsible for the transport of exogenous lactate into PK-15 cells (MO) (Figures S3A and S3B and, Table 1, S1, and S2). As shown in Figures 3E and 3F, the deletion of the *MCT1* gene itself had no effect on CSFV replication or intracellular lactate levels. However, exogenous lactate could not restore CSFV replication or intracellular lactate levels by knocking out *PFKL* (PMO) and *LDHA* (LMO) on the basis of *MCT1* and knockout (Figures 3G–3I). Collectively, intracellular, but not extracellular, lactate promotes CSFV replication.

Lactate promotes cholesterol biosynthesis to maintain the replication of CSFV

When compared with the control group, along with lactate reduction, cholesterol was decreased in the LO cells, and the exogenous addition of cholesterol, similar to lactate addition, reversed the inhibition of CSFV replication in the LO cells. Moreover, the increased total SREBP2 protein in CSFV-infected cells was reduced when *LDHA* was deleted. The addition of lactate could reverse SREBP2 and cholesterol reductions in the LO cells. (Figures 4A, 4B, and 4D). However, exogenous cholesterol could not restore intracellular lactate and SREBP2 protein levels in the LO cells (Figures 4C and 4D). Then, the *SQLE* gene was deleted, a key enzyme in cholesterol biosynthesis, to investigate the relationship between intracellular lactate and cholesterol biosynthesis (Figures S4A and S4B). In the *SQLE*-deleted cells (SO), CSFV replication and intracellular cholesterol levels were significantly reduced. However, exogenous lactate could not be used to reverse CSFV replication and intracellular cholesterol levels (Figures 4E and 4F and Table 1). Taken together, cholesterol mediates the effect of lactate on CSFV replication.

Cholesterol biosynthesis mediates the lactate effects on type I IFN response in CSFV-infected PK-15 cells

Interferons (IFNs) have been found to have a stronger link to glycolysis. Simultaneously, another study discovered that restricting flux through the cholesterol biosynthetic pathway triggered a type I IFN

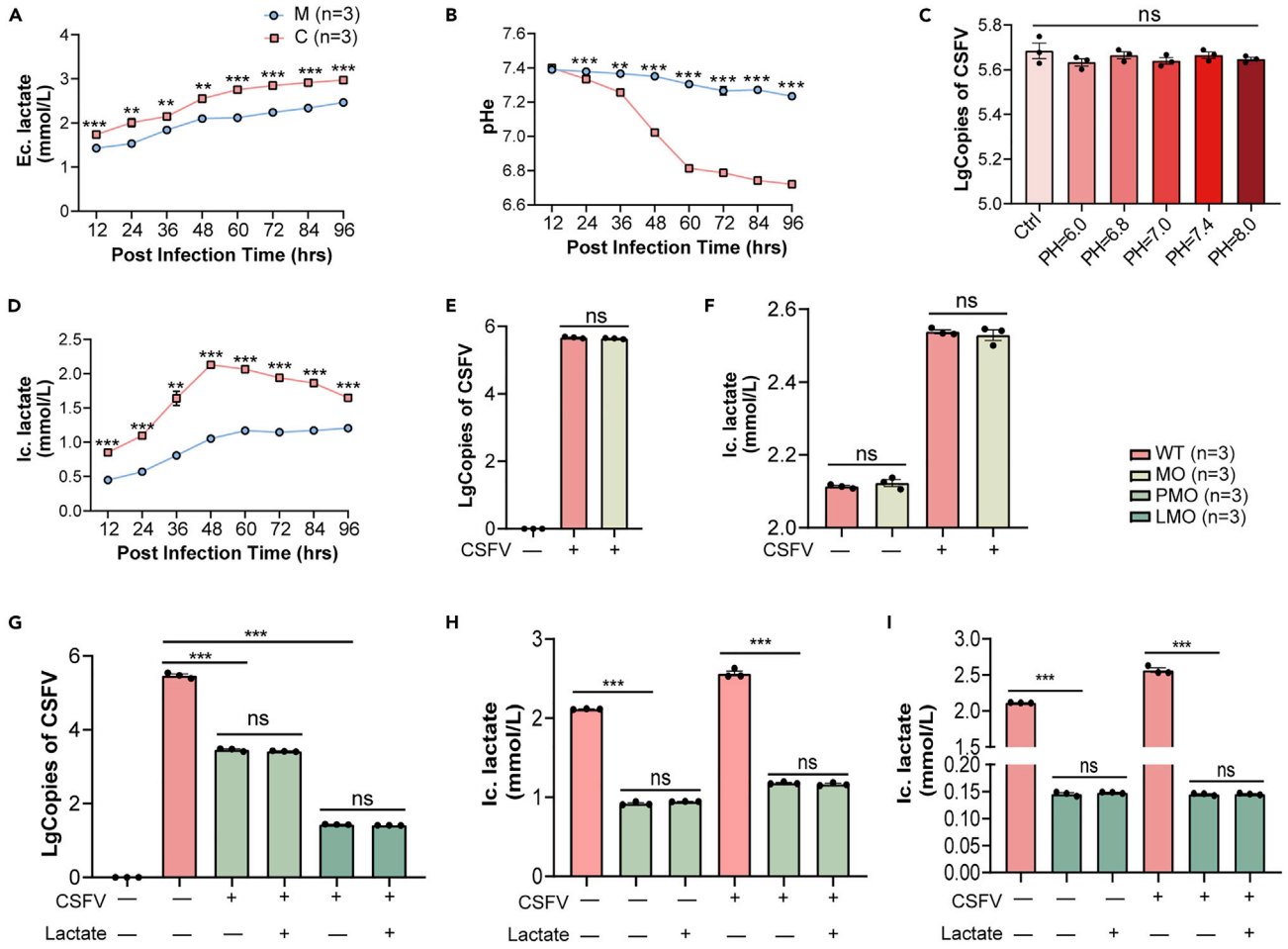

Figure 3. Intracellular lactate plays a role in CSFV replication

(A and D) The alterations of extracellular and intracellular lactate levels in CSFV-infected PK-15 cells within 96 hpi, n = 3, **p < 0.01, ***p < 0.001.

(B) The alteration curve of pH for CSFV-infected PK-15 cells within 96 hpi, n = 3, **p < 0.01, ***p < 0.001.

(C) CSFV replication was unaffected by different pH levels, n = 3, ns, no significance.

(E and F) CSFV replication and intracellular lactate levels in PK-15 cells were unaffected by the deletion of the *MCT1* gene，ns, no significance.

(G–I) CSFV replication and intracellular lactate levels in PMO and LMO cells could not be reversed by lactate treatment, n = 3, ***p < 0.001. (WT, wild-type; MO, mct1-ko; PMO, pfkl&mct1-ko; LMO, ldha&mct1-ko; Ec. lactate, extracellular lactate level; Ic. lactate, intracellular lactate level.)

response in a STING-dependent manner (Fritsch and Weichhart, 2016; York et al., 2015). Thus, we investigated the roles of cholesterol on the regulation of glycolysis via IFNs during CSFV replication. As shown in Figures 5A–5H and S5A–S5H, the levels of phosphorylated TBK1 (p-TBK1) and interferon-stimulated genes (ISGs) such as *CCL2*, *CXCL10*, and *MX1* in CSFV-infected PK-15 cells were significantly suppressed at 48 hpi. Disruption of glycolysis or the cholesterol biosynthesis pathway both facilitated the expression of p-TBK1 and ISGs. Exogenous lactate and cholesterol could both restore p-TBK1 and ISG levels in the LO cells. However, only the addition of cholesterol, rather than lactate, was able to reverse p-TBK1 and ISG expression in the SO cells. Collectively, these data suggest that CSFV infection enhances aerobic glycolysis to produce a large amount of lactate that activates cholesterol biosynthesis to attenuate type I IFN signaling.

DISCUSSION

In this study, we showed that CSFV infection enhanced aerobic glycolysis in PK-15 cells and the end product of glycolysis, i.e., lactate, was the essential molecule that maintained CSFV replication. Meanwhile, lactate accumulation promoted the synthesis of cholesterol, which disrupted the type I IFN response and further facilitated CSFV replication.

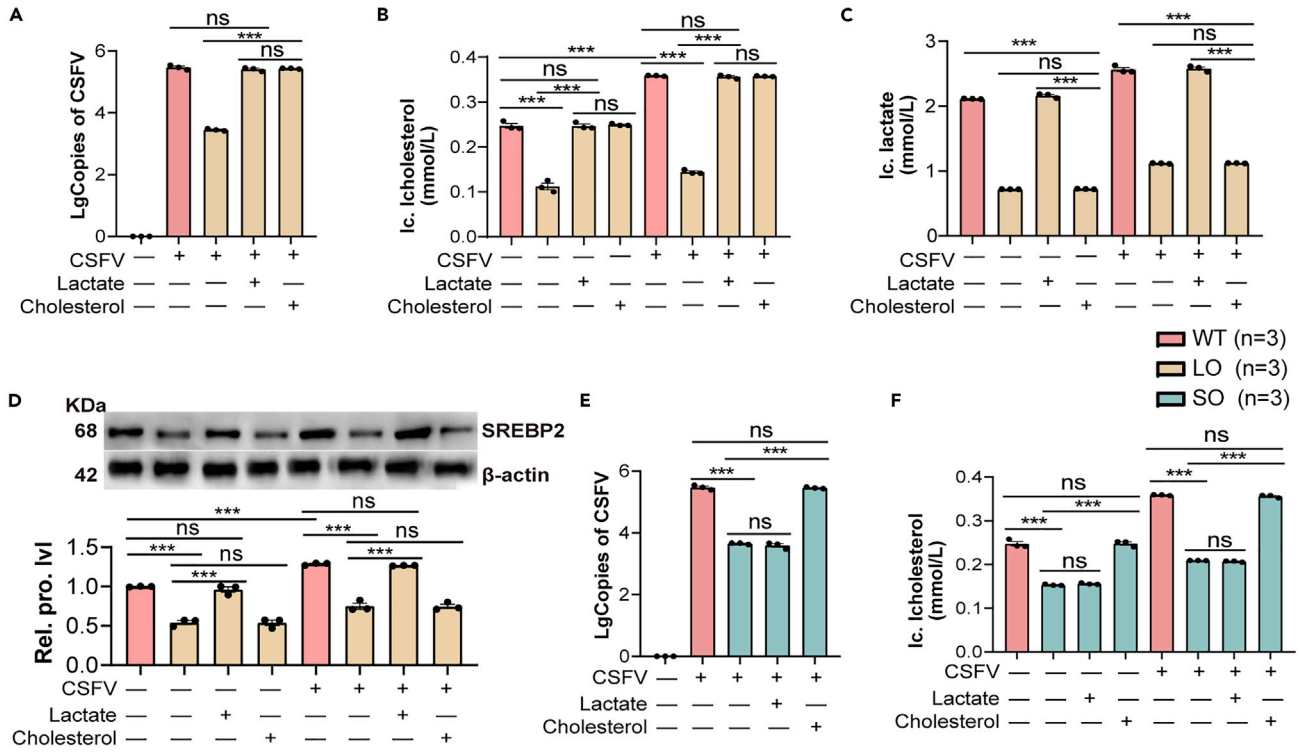

Figure 4. Intracellular lactate promotes cholesterol biosynthesis

(A and E) The number of viral genomic RNA copies was determined by qPCR, n = 3, ***p < 0.001.

(B) The addition of cholesterol had the same effect as lactate in restoring intracellular cholesterol levels in LO cells, n = 3, ***p < 0.001.

(C) The addition of lactate could restore the lactate level in LO cells, n = 3, ***p < 0.001.

(D) The levels of protein expression of SREBP2, n = 3, ***p < 0.001.

(F) Lactate could not be used to reverse intracellular cholesterol levels in SO cells during CSFV replication, n = 3, ***p < 0.001. (WT, wild-type; LO, ldha-ko; SO, sqle-ko; Rel. expr. lvl, relative expression level; Rel. prot. lvl, relative protein level; Ec. lactate, extracellular lactate level; Ic. lactate, intracellular lactate level; Ic. cholesterol, intracellular cholesterol level.)

Accumulating evidence has suggested that a virus and its encoded genes or proteins alter host cell metabolism by modifying the expression and activity of glucose transporters and glycolytic enzymes and modulating the function of key signaling molecules involved in host cell metabolism for viral replication (Yu et al., 2018). The adenoviral gene product E4ORF1 enhances MYC transcriptional activity to upregulate glycolytic target genes such as *HK2*, *LDHA*, and *PFK1* for optimal adenovirus replication (Thai et al., 2014). DENV nonstructural protein 1 (NS1) enhances glycolysis flux and energy production by suppressing the function of GAPDH (Allonso et al., 2015; Silva et al., 2019). EBV-encoded LMP1 activates the FGFR1 signaling pathway to increase the cellular uptake of glucose and to enhance LDHA activity and regulates HoxC8 expression via PolII stalling to stabilize the expression of glycolytic genes such as *GLUT1* and *HK2* (Jiang et al., 2015; Lo et al., 2015). In addition, C-terminal-activating regions of LMP1 can promote GLUT1 transcription via the mTORC1/NF-κB signaling pathway (Zhang et al., 2017). The hepatitis B virus core protein (HBc) and x protein (HBx) can increase key glycolytic enzymes and related genes *NAMPT* and *NRF2* to enhance glycolysis (Guo et al., 2021; Xie et al., 2017). Moreover, HCV severely impairs mitochondrial oxidative phosphorylation to promote HIF-1α expression and transcriptional activation, and its encoded proteins (NS5A and NS5B) can promote glycolytic enzymes' activity to enhance glycolysis for viral replication (Ramière et al., 2014; Ripoli et al., 2010; Wu et al., 2008). Previous studies have used 2D polyacrylamide gel electrophoresis followed by MALDI-TOF tandem mass spectromentry identification to perform proteomic analyses in CSFV-infected PK-15 cells and have found that CSFV replication affects glycolytic enzyme expression including upregulated (PGAM1), triosephosphate isomerase, and downregulated GAPDH in PK-15 cells (Gou et al., 2017). However, in CSFV-infected PK-15 cells, a metabolic analysis revealed that CSFV replication decreased glycolytic intermediates such as glucose 6-phosphate (FC = −1.94) and glyceraldehyde-3-phosphate (FC = −1.83) (Sun et al., 2008). In our study, increased glucose consumption, lactate production,

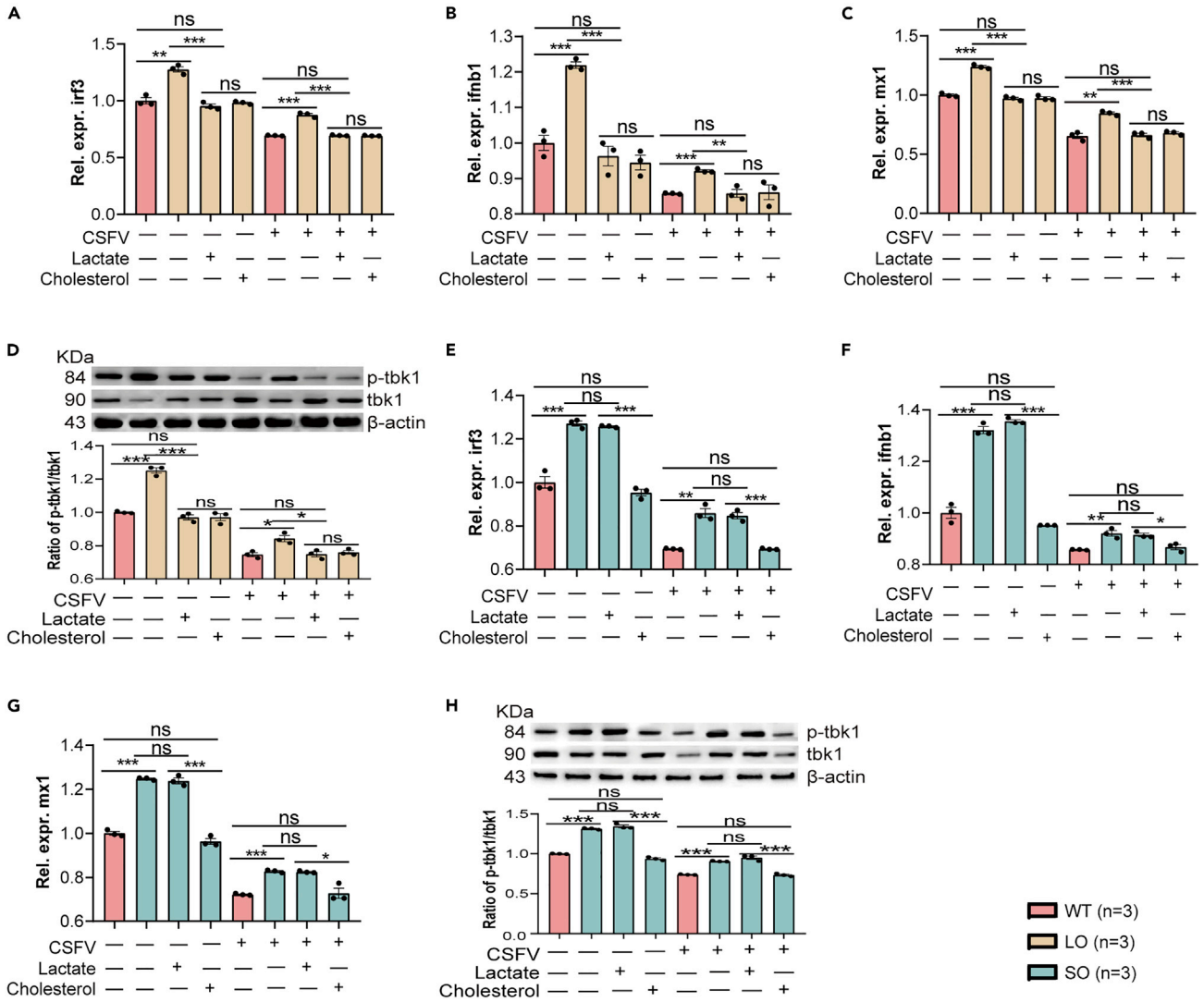

Figure 5. Intracellular lactate promotes cholesterol biosynthesis for inhibiting activation of type I IFN signal pathway during CSFV replication

(A–D) In CSFV-infected PK-15 cells, disrupting glycolysis could increase the expression of ISGs and p-TBK1, whereas treating with lactate could reverse this phenomenon, n = 3, *p < 0.05, **p < 0.01, ***p < 0.001.

(E–H) The absence of the *SQLE* gene increased ISG and p-TBK1 expression, which was not reversed by lactate. The addition of cholesterol could reverse these effects, n = 3, *p < 0.05, **p < 0.01***p < 0.001. (WT, wild-type; LO, ldha-ko; SO, sqle-ko; Rel. expr. lvl, relative expression level; Rel. prot. lvl, relative protein level.)

and the expression of glucose transporter GLUT1 and the glycolytic enzyme LDHA were also found in CSFV-infected PK-15 cells. The transcriptome results further confirmed that the glycolytic flux was significantly enhanced in CSFV-infected cells when compared with the control group. Inhibition of the tricarboxylic acid (TCA) cycle or addition of lactate in PFKL or LDHA knockout (KO) cells both increased CSFV replication. The data confirmed the relationship between glycolysis flux or lactate and CSFV replication.

Previous research has reported that the accumulation of lactate contributed to the acidification of a tumor microenvironment, and that the acidosis favored metastasis, angiogenesis, and immunosuppression (de la Cruz-Lopez et al., 2019). In the present study, we employed various pH values using the addition of lactate to observe the effect on CSFV replication. The data demonstrated that lactate, and not the acidic environment, maintained CSFV replication. When MCT1 was deleted, which blocked the transportation of exogenous materials into cells, especially lactate, which is the predominant carbon source of TCA, the CSFV replication was not affected. Thus, endogenous lactate is sufficient to support the replication of CSFV.

It is well known that the glycolytic intermediate, glucose-6-phosphate, can promote the pentose phosphate pathway (PPP), and the enhanced PPP produces pentoses, which is used to synthesize DNA, RNA, and co-factors in enzymes. In cancer, aerobic glycolysis provides cellular energy, and also increases PPP to process macromolecular biosynthesis, conferring a selective advantage under diminished nutrition (Patra and Hay, 2014). However, in the present study, PFKL KO, which forced PPP enhancement, blocked lactate production and the TCA cycle, and still decreased CSFV replication significantly, similar to that of LDHA KO, which blocked lactate production and enhanced the TCA cycle. The data demonstrated that neither PPP nor the TCA cycle was the determinant factor, and lactate played an essential role in CSFV replication.

How does lactate maintain CSFV replication? Numerous reports have indicated that lipid metabolism plays an important role during the viral replication cycle (Monson et al., 2021). HIV, via its accessory protein Nef, downregulates ATP-binding cassette transporter A1 (ABCA1) expression and alters intracellular distribution of ABCA1, thus consequently impairing cholesterol efflux of infected macrophages and increasing infectivity of HIV virions (Mujawar et al., 2006). DENV infection induces autophagy, causing the depletion of LD triglyceride stores and the release of free fatty acids, and facilitates robust viral RNA replication (Heaton and Randall, 2010). HBx induces the expression of liver x receptor (LXR) and its lipogenic target genes such as sterol regulatory element-binding protein-1c (SREBP-1c), and this is accompanied by the accumulation of LDs (Na et al., 2009). HCV and its viral proteins such as core, NS2, and NS4B modulate lipid homeostasis by increasing lipogenesis via SREBP activation and reducing oxidation and lipid export (Moriishi et al., 2007; Negro and Sanyal, 2009; Oem et al., 2008; Park et al., 2009). Regarding CSFV, many studies have demonstrated that interference with cholesterol biosynthesis and trafficking affected its life cycle (Liang et al., 2019; Yu et al., 2019; Zou et al., 2022). In the present study, we observed that exogenous lactate could increase either CSFV replication or intracellular cholesterol level in LDHA KO cells. Moreover, LDHA KO-induced CSFV replication could be elevated by cholesterol addition. Furthermore, lactate could not enhance CSFV replication when the synthesis of cholesterol was disrupted. Collectively, CSFV-induced lactate production enhances cholesterol biosynthesis, which facilitates the replication of itself.

Current mechanistic studies have revealed that limiting the cholesterol biosynthetic pathway spontaneously engaged a type I IFN response in a STING-dependent manner (York et al., 2015). Meanwhile, studies have showed that lactate inhibited retinoic acid-inducible gene I (RIG-I)-like receptor (RLR) signaling, resulting in decreased type I interferon production and viral clearance (Zhang et al., 2019). Our data also showed that CSFV infection induced lactate accumulation, which disturbed the type I IFN response by altering the cholesterol level in PK-15 cells.

In conclusion, our findings show that CSFV infection induces reprogramming of host cell metabolism, which facilitates its replication. Mechanistically, the aerobic glycolysis induced by CSFV infection enhances the accumulation of lactate in cells, and the lactate promotes cholesterol biosynthesis, which facilitates the replication of CSFV and disrupts the type I IFN response.

Limitations of the study

Although our study highlights that lactate promotes cholesterol biosynthesis to facilitate CSFV replication, several limitations of our study remain to be explored that will further shed light on detailed mechanism of action, for example, experiments probing how lactate regulates cholesterol biosynthesis and its mechanism. We believe these are important future research avenues that will elucidate the exact mechanism of action of lactate in CSFV replication.

STAR★METHODS

Detailed methods are provided in the online version of this paper and include the following:

- KEY RESOURCES TABLE
- RESOURCE AVAILABILITY
  - Lead contact
  - Materials availability
  - Data and code availability
- EXPERIMENTAL MODEL AND SUBJECT DETAILS
  - Cell lines
  - Virus strain

SUPPLEMENTAL INFORMATION

Supplemental information can be found online at https://doi.org/10.1016/j.isci.2022.105353.

ACKNOWLEDGMENTS

This work was financially supported by the National Natural Science Foundation of China (no. 31972710 and 31772747). We thank our colleagues from the College of Animal Sciences, Jilin University, for their discussion and feedback.

AUTHOR CONTRIBUTIONS

X.Z., H.O., D.P., and X.T. conceived the study and wrote the manuscript. X.Z., Y.Y., F.L., J.C., H.Z., and L.L. performed the experiments, analyzed the data, and drafted the manuscript. L.R. reviewed and revised the manuscript.

DECLARATION OF INTERESTS

The authors declare that they have no conflicts of interest.

Received: May 11, 2022
Revised: September 14, 2022
Accepted: October 11, 2022
Published: November 18, 2022

REFERENCES

Ajaz, S., McPhail, M.J., Singh, K.K., Mujib, S., Trovato, F.M., Napoli, S., and Agarwal, K. (2021). Mitochondrial metabolic manipulation by SARS-CoV-2 in peripheral blood mononuclear cells of patients with COVID-19. Am. J. Physiol. Cell Physiol. *320*, C57–C65. https://doi.org/10.1152/ajpcell.00426.2020.

Allonso, D., Andrade, I.S., Conde, J.N., Coelho, D.R., Rocha, D.C., da Silva, M.L., Ventura, G.T., Silva, E.M., and Mohana-Borges, R. (2015). Dengue virus NS1 protein modulates cellular energy metabolism by increasing glyceraldehyde-3-phosphate dehydrogenase activity. J. Virol. *89*, 11871–11883. https://doi.org/10.1128/jvi.01342-15.

Becker, H.M. (2020). Carbonic anhydrase IX and acid transport in cancer. Br. J. Cancer *122*, 157–167. https://doi.org/10.1038/s41416-019-0642-z.

Cheung, W., Gill, M., Esposito, A., Kaminski, C.F., Courousse, N., Chwetzoff, S., Trugnan, G., Keshavan, N., Lever, A., and Desselberger, U. (2010). Rotaviruses associate with cellular lipid droplet components to replicate in viroplasms, and compounds disrupting or blocking lipid droplets inhibit viroplasm formation and viral replication. J. Virol. *84*, 6782–6798. https://doi.org/10.1128/jvi.01757-09.

de la Cruz-López, K.G., Castro-Muñoz, L.J., Reyes-Hernández, D.O., García-Carrancá, A., and Manzo-Merino, J. (2019). Lactate in the regulation of tumor microenvironment and Therapeutic approaches. Front. Oncol. *9*, 1143. https://doi.org/10.3389/fonc.2019.01143.

Dias, S.S.G., Soares, V.C., Ferreira, A.C., Sacramento, C.Q., Fintelman-Rodrigues, N., Temerozo, J.R., Teixeira, L., Nunes da Silva, M.A., Barreto, E., Mattos, M., et al. (2020). Lipid droplets fuel SARS-CoV-2 replication and production of inflammatory mediators. PLoS Pathog. *16*, e1009127. https://doi.org/10.1371/journal.ppat.1009127.

Episcopio, D., Aminov, S., Benjamin, S., Germain, G., Datan, E., Landazuri, J., Lockshin, R.A., and Zakeri, Z. (2019). Atorvastatin restricts the ability of influenza virus to generate lipid droplets and severely suppresses the replication of the virus. Faseb. J. *33*, 9516–9525. https://doi.org/10.1096/fj.201900428RR.

Fritsch, S.D., and Weichhart, T. (2016). Effects of interferons and viruses on metabolism. Front. Immunol. *7*, 630. https://doi.org/10.3389/fimmu.2016.00630.

Gou, H., Zhao, M., Yuan, J., Xu, H., Ding, H., and Chen, J. (2017). Metabolic profiles in cell lines infected with classical swine fever virus. Front. Microbiol. *8*, 691. https://doi.org/10.3389/fmicb.2017.00691.

Gualdoni, G.A., Mayer, K.A., Kapsch, A.M., Kreuzberg, K., Puck, A., Kienzl, P., Oberndorfer, F., Frühwirth, K., Winkler, S., Blaas, D., et al. (2018). Rhinovirus induces an anabolic reprogramming in host cell metabolism essential for viral replication. Proc. Natl. Acad. Sci. USA *115*, E7158–E7165. https://doi.org/10.1073/pnas.1800525115.

Guo, H.J., Li, H.Y., Chen, Z.H., Zhou, W.J., Li, J.J., Zhang, J.Y., Wang, J., Luo, X.Y., Zeng, T., Shi, Z., and Mo, C.F. (2021). NAMPT promotes hepatitis B virus replication and liver cancer cell proliferation through the regulation of aerobic glycolysis. Oncol. Lett. *21*, 390. https://doi.org/10.3892/ol.2021.12651.

Heaton, N.S., and Randall, G. (2010). Dengue virus-induced autophagy regulates lipid metabolism. Cell Host Microbe *8*, 422–432. https://doi.org/10.1016/j.chom.2010.10.006.

Hou, W., Cruz-Cosme, R., Armstrong, N., Obwolo, L.A., Wen, F., Hu, W., Luo, M.H., and Tang, Q. (2017). Molecular cloning and characterization of the genes encoding the proteins of Zika virus. Gene *628*, 117–128. https://doi.org/10.1016/j.gene.2017.07.049.

Hulse, M., Johnson, S.M., Boyle, S., Caruso, L.B., and Tempera, I. (2021). Epstein-barr virus-encoded latent membrane protein 1 and B-cell growth transformation induce lipogenesis through fatty acid synthase. J. Virol. *95*, 018577–e1920. https://doi.org/10.1128/jvi.01857-20.

Ji, W., Guo, Z., Ding, N.Z., and He, C.Q. (2015). Studying classical swine fever virus: making the best of a bad virus. Virus Res. *197*, 35–47. https://doi.org/10.1016/j.virusres.2014.12.006.

Jiang, Y., Yan, B., Lai, W., Shi, Y., Xiao, D., Jia, J., Liu, S., Li, H., Lu, J., Li, Z., et al. (2015). Repression of Hox genes by LMP1 in nasopharyngeal carcinoma and modulation of glycolytic pathway genes by HoxC8. Oncogene *34*, 6079–6091. https://doi.org/10.1038/onc.2015.53.

Kapadia, S.B., and Chisari, F.V. (2005). Hepatitis C virus RNA replication is regulated by host geranylgeranylation and fatty acids. Proc. Natl. Acad. Sci. USA *102*, 2561–2566. https://doi.org/10.1073/pnas.0409834102.

Kato, Y., Ozawa, S., Miyamoto, C., Maehata, Y., Suzuki, A., Maeda, T., and Baba, Y. (2013). Acidic extracellular microenvironment and cancer. Cancer Cell Int. *13*, 89. https://doi.org/10.1186/1475-2867-13-89.

Liang, X.D., Zhang, Y.N., Liu, C.C., Chen, J., Chen, X.N., Sattar Baloch, A., and Zhou, B. (2019). U18666A inhibits classical swine fever virus replication through interference with intracellular cholesterol trafficking. Vet. Microbiol. *238*, 108436. https://doi.org/10.1016/j.vetmic.2019.108436.

Lo, A.K.F., Dawson, C.W., Young, L.S., Ko, C.W., Hau, P.M., and Lo, K.W. (2015). Activation of the FGFR1 signalling pathway by the Epstein-Barr virus-encoded LMP1 promotes aerobic glycolysis and transformation of human nasopharyngeal epithelial cells. J. Pathol. *237*, 238–248. https://doi.org/10.1002/path.4575.

Lyu, X., Wang, J., Guo, X., Wu, G., Jiao, Y., Faleti, O.D., Liu, P., Liu, T., Long, Y., Chong, T., et al. (2018). EBV-miR-BART1-5P activates AMPK/mTOR/HIF1 pathway via a PTEN independent manner to promote glycolysis and angiogenesis in nasopharyngeal carcinoma. PLoS Pathog. *14*, e1007484. https://doi.org/10.1371/journal.ppat.1007484.

Martins, A.S., Carvalho, F.A., Faustino, A.F., Martins, I.C., and Santos, N.C. (2019). West Nile virus capsid protein interacts with biologically relevant host lipid systems. Front. Cell. Infect. Microbiol. *9*, 8. https://doi.org/10.3389/fcimb.2019.00008.

Mayer, K.A., Stöckl, J., Zlabinger, G.J., and Gualdoni, G.A. (2019). Hijacking the supplies: metabolism as a novel facet of virus-host interaction. Front. Immunol. *10*, 1533. https://doi.org/10.3389/fimmu.2019.01533.

Monson, E.A., Trenerry, A.M., Laws, J.L., Mackenzie, J.M., and Helbig, K.J. (2021). Lipid droplets and lipid mediators in viral infection and immunity. FEMS Microbiol. Rev. *45*, fuaa066. https://doi.org/10.1093/femsre/fuaa066.

Moriishi, K., Mochizuki, R., Moriya, K., Miyamoto, H., Mori, Y., Abe, T., Murata, S., Tanaka, K., Miyamura, T., Suzuki, T., et al. (2007). Critical role of PA28gamma in hepatitis C virus-associated steatogenesis and hepatocarcinogenesis. Proc. Natl. Acad. Sci. USA *104*, 1661–1666. https://doi.org/10.1073/pnas.0607312104.

Mujawar, Z., Rose, H., Morrow, M.P., Pushkarsky, T., Dubrovsky, L., Mukhamedova, N., Fu, Y., Dart, A., Orenstein, J.M., Bobryshev, Y.V., et al. (2006). Human immunodeficiency virus impairs reverse cholesterol transport from macrophages. PLoS Biol. *4*, e365. https://doi.org/10.1371/journal.pbio.0040365.

Na, T.Y., Shin, Y.K., Roh, K.J., Kang, S.A., Hong, I., Oh, S.J., Seong, J.K., Park, C.K., Choi, Y.L., and Lee, M.O. (2009). Liver X receptor mediates hepatitis B virus X protein-induced lipogenesis in hepatitis B virus-associated hepatocellular carcinoma. Hepatology *49*, 1122–1131. https://doi.org/10.1002/hep.22740.

Negro, F., and Sanyal, A.J. (2009). Hepatitis C virus, steatosis and lipid abnormalities: clinical and pathogenic data. Liver Int. *29* (*Suppl 2*), 26–37. https://doi.org/10.1111/j.1478-3231.2008.01950.x.

Oem, J.K., Jackel-Cram, C., Li, Y.P., Zhou, Y., Zhong, J., Shimano, H., Babiuk, L.A., and Liu, Q. (2008). Activation of sterol regulatory element-binding protein 1c and fatty acid synthase transcription by hepatitis C virus non-structural protein 2. J. Gen. Virol. *89*, 1225–1230. https://doi.org/10.1099/vir.0.83491-0.

Ohol, Y.M., Wang, Z., Kemble, G., and Duke, G. (2015). Direct inhibition of cellular fatty acid synthase impairs replication of respiratory syncytial virus and other respiratory viruses. PLoS One *10*, e0144648. https://doi.org/10.1371/journal.pone.0144648.

Park, C.Y., Jun, H.J., Wakita, T., Cheong, J.H., and Hwang, S.B. (2009). Hepatitis C virus nonstructural 4B protein modulates sterol regulatory element-binding protein signaling via the AKT pathway. J. Biol. Chem. *284*, 9237–9246. https://doi.org/10.1074/jbc.M808773200.

Passalacqua, K.D., Lu, J., Goodfellow, I., Kolawole, A.O., Arche, J.R., Maddox, R.J., Carnahan, K.E., O'Riordan, M.X.D., and Wobus, C.E. (2019). Glycolysis is an intrinsic factor for optimal replication of a norovirus. mBio *10*, 021755–e2218. https://doi.org/10.1128/mBio.02175-18.

Patra, K.C., and Hay, N. (2014). The pentose phosphate pathway and cancer. Trends Biochem. Sci. *39*, 347–354. https://doi.org/10.1016/j.tibs.2014.06.005.

Ramière, C., Rodriguez, J., Enache, L.S., Lotteau, V., André, P., and Diaz, O. (2014). Activity of hexokinase is increased by its interaction with hepatitis C virus protein NS5A. J. Virol. *88*, 3246–3254. https://doi.org/10.1128/jvi.02862-13.

Ripoli, M., D'Aprile, A., Quarato, G., Sarasin-Filipowicz, M., Gouttenoire, J., Scrima, R., Cela, O., Boffoli, D., Heim, M.H., Moradpour, D., et al. (2010). Hepatitis C virus-linked mitochondrial dysfunction promotes hypoxia-inducible factor 1 alpha-mediated glycolytic adaptation. J. Virol. *84*, 647–660. https://doi.org/10.1128/jvi.00769-09.

Samsa, M.M., Mondotte, J.A., Iglesias, N.G., Assunção-Miranda, I., Barbosa-Lima, G., Da Poian, A.T., Bozza, P.T., and Gamarnik, A.V. (2009). Dengue virus capsid protein usurps lipid droplets for viral particle formation. PLoS Pathog. *5*, e1000632. https://doi.org/10.1371/journal.ppat.1000632.

Silva, E.M., Conde, J.N., Allonso, D., Ventura, G.T., Coelho, D.R., Carneiro, P.H., Silva, M.L., Paes, M.V., Rabelo, K., Weissmuller, G., et al. (2019). Dengue virus nonstructural 3 protein interacts directly with human glyceraldehyde-3-phosphate dehydrogenase (GAPDH) and reduces its glycolytic activity. Sci. Rep. *9*, 2651. https://doi.org/10.1038/s41598-019-39157-7.

Singh, S., Singh, P.K., Suhail, H., Arumugaswami, V., Pellett, P.E., Giri, S., and Kumar, A. (2020). AMP-activated protein kinase restricts Zika virus replication in endothelial cells by potentiating innate antiviral responses and inhibiting glycolysis. J. Immunol. *204*, 1810–1824. https://doi.org/10.4049/jimmunol.1901310.

Sorbara, L.R., Maldarelli, F., Chamoun, G., Schilling, B., Chokekijcahi, S., Staudt, L., Mitsuya, H., Simpson, I.A., and Zeichner, S.L. (1996). Human immunodeficiency virus type 1 infection of H9 cells induces increased glucose transporter expression. J. Virol. *70*, 7275–7279. https://doi.org/10.1128/jvi.70.10.7275-7279.1996.

Spencer, C.M., Schafer, X.L., Moorman, N.J., and Munger, J. (2011). Human cytomegalovirus induces the activity and expression of acetyl-coenzyme A carboxylase, a fatty acid biosynthetic enzyme whose inhibition attenuates viral replication. J. Virol. *85*, 5814–5824. https://doi.org/10.1128/jvi.02630-10.

Sumbria, D., Berber, E., Mathayan, M., and Rouse, B.T. (2020). Virus infections and host metabolism-can we manage the interactions? Front. Immunol. *11*, 594963. https://doi.org/10.3389/fimmu.2020.594963.

Sun, J., Jiang, Y., Shi, Z., Yan, Y., Guo, H., He, F., and Tu, C. (2008). Proteomic alteration of PK-15 cells after infection by classical swine fever virus. J. Proteome Res. *7*, 5263–5269. https://doi.org/10.1021/pr800546m.

Thai, M., Graham, N.A., Braas, D., Nehil, M., Komisopoulou, E., Kurdistani, S.K., McCormick, F., Graeber, T.G., and Christofk, H.R. (2014). Adenovirus E4ORF1-induced MYC activation promotes host cell anabolic glucose metabolism and virus replication. Cell Metab. *19*, 694–701. https://doi.org/10.1016/j.cmet.2014.03.009.

Thaker, S.K., Ch'ng, J., and Christofk, H.R. (2019). Viral hijacking of cellular metabolism. BMC Biol. *17*, 59. https://doi.org/10.1186/s12915-019-0678-9.

Varanasi, S.K., and Rouse, B.T. (2018). How host metabolism impacts on virus pathogenesis. Curr. Opin. Virol. *28*, 37–42. https://doi.org/10.1016/j.coviro.2017.11.003.

Vogt, D.A., Camus, G., Herker, E., Webster, B.R., Tsou, C.L., Greene, W.C., Yen, T.S.B., and Ott, M. (2013). Lipid droplet-binding protein TIP47 regulates hepatitis C Virus RNA replication through interaction with the viral NS5A protein. PLoS Pathog. *9*, e1003302. https://doi.org/10.1371/journal.ppat.1003302.

Wilsky, S., Sobotta, K., Wiesener, N., Pilas, J., Althof, N., Munder, T., Wutzler, P., and Henke, A. (2012). Inhibition of fatty acid synthase by amentoflavone reduces coxsackievirus B3 replication. Arch. Virol. *157*, 259–269. https://doi.org/10.1007/s00705-011-1164-z.

Wu, X., Zhou, Y., Zhang, K., Liu, Q., and Guo, D. (2008). Isoform-specific interaction of pyruvate kinase with hepatitis C virus NS5B. FEBS Lett. *582*, 2155–2160. https://doi.org/10.1016/j.febslet.2008.05.033.

Xie, Q., Fan, F., Wei, W., Liu, Y., Xu, Z., Zhai, L., Qi, Y., Ye, B., Zhang, Y., Basu, S., et al. (2017). Multi-omics analyses reveal metabolic alterations regulated by hepatitis B virus core protein in hepatocellular carcinoma cells. Sci. Rep. *7*, 41089. https://doi.org/10.1038/srep41089.

York, A.G., Williams, K.J., Argus, J.P., Zhou, Q.D., Brar, G., Vergnes, L., Gray, E.E., Zhen, A., Wu, N.C., Yamada, D.H., et al. (2015). Limiting cholesterol biosynthetic flux spontaneously engages type I IFN signaling. Cell *163*, 1716–1729. https://doi.org/10.1016/j.cell.2015.11.045.

Yu, L., Chen, X., Wang, L., and Chen, S. (2018). Oncogenic virus-induced aerobic glycolysis and tumorigenesis. J. Cancer *9*, 3699–3706. https://doi.org/10.7150/jca.27279.

Yu, S., Yin, C., Song, K., Li, S., Zheng, G.L., Li, L.F., Wang, J., Li, Y., Luo, Y., Sun, Y., and Qiu, H.J. (2019). Engagement of cellular cholesterol in the life cycle of classical swine fever virus: its potential as an antiviral target. J. Gen. Virol. *100*, 156–165. https://doi.org/10.1099/jgv.0.001178.

Yuan, S., Chu, H., Chan, J.F.W., Ye, Z.W., Wen, L., Yan, B., Lai, P.M., Tee, K.M., Huang, J., Chen, D., et al. (2019). SREBP-dependent lipidomic reprogramming as a broad-spectrum antiviral target. Nat. Commun. *10*, 120. https://doi.org/10.1038/s41467-018-08015-x.

Zhang, J., Jia, L., Lin, W., Yip, Y.L., Lo, K.W., Lau, V.M.Y., Zhu, D., Tsang, C.M., Zhou, Y., Deng, W., et al. (2017). Epstein-barr virus-encoded latent membrane protein 1 upregulates glucose transporter 1 transcription via the mTORC1/NF-κB signaling pathways. J. Virol. *91*, 021688–e2216. https://doi.org/10.1128/jvi.02168-16.

Zhang, W., Wang, G., Xu, Z.G., Tu, H., Hu, F., Dai, J., Chang, Y., Chen, Y., Lu, Y., Zeng, H., et al. (2019). Lactate is a natural suppressor of RLR signaling by targeting MAVS. Cell *178*, 176–189.e15. https://doi.org/10.1016/j.cell.2019.05.003.

Zhou, Y., Zhou, B., Pache, L., Chang, M., Khodabakhshi, A.H., Tanaseichuk, O., Benner, C., and Chanda, S.K. (2019). Metascape provides a biologist-oriented resource for the analysis of systems-level datasets. Nat. Commun. *10*, 1523. https://doi.org/10.1038/s41467-019-09234-6.

Zou, X., Lin, F., Yang, Y., Chen, J., Zhang, H., Li, L., Ouyang, H., Pang, D., and Tang, X. (2022). Cholesterol biosynthesis modulates CSFV replication. Viruses *14*. https://doi.org/10.3390/v14071450.

STAR★METHODS

KEY RESOURCES TABLE

REAGENT or RESOURCE	SOURCE	IDENTIFIER
Antibodies		
Anti-SLC2A1 Antibody	BOSTER	RRID: AB_PB9435
Anti-GCK Antibody	BOSTER	RRID: AB_A00884-1
Anti-LDHA Antibody	BOSTER	RRID: AB_PB10075
Anti-SLC16A4 Antibody	BOSTER	RRID: AB_BA3245
Phospho-TBK1/NAK Antibody	Beyotime	RRID: AB_AF5959
TBK1 Rabbit Polyclonal Antibody	Beyotime	RRID: AB_AF8103
β-Actin Mouse Monoclonal Antibody	Beyotime	Cat# AF0003 ; RRID:AB_2893353
HRP-labeled Goat Anti-Mouse IgG(H + L)	Beyotime	Cat# A0216 ; RRID:AB_2860575
HRP-labeled Goat Anti-Rabbit IgG(H + L)	Beyotime	Cat# A0208 ; RRID:AB_2892644
PFKM Polyclonal antibody	Proteintech	Cat# 55028-1-AP ; RRID:AB_10858390
Bacterial and virus strains		
CSFV (Shimen strain)	Academy of Military Medical Sciences, Changchun, China	Dr. Changchun Tu
Chemicals, peptides, and recombinant proteins		
2-Deoxy-D-glucose (2-DG)	MCE	HY-13966
UK-5099	MCE	HY-15475
Lactate	Sigma	50-21-5
Cholesterol	Sigma	C8667
Critical commercial assays		
Tissue Cell Glucose Oxidase Assay	Pplygen	E1011
Lactate assay kit	Nanjing Jiancheng Bioengineering Institute	A019-2-1
Total cholesterol assay kit	Nanjing Jiancheng Bioengineering Institute	A111-1-1
Cell Counting Kit-8 assay	Dojindo	CK04
BCA Protein Assay Kit	Beyotime	P0010
Enhanced ATP Assay Kit	Beyotime	S0027
TRNzol-A + Reagent	Tiangen	DP424
FastKing RT Kit (with gDNase)	Tiangen	KR116
ChamQ Universal SYBR qPCR Master Mix	Vazyme	Q711-02
Experimental models: Cell lines		
PK-15	ATCC	CCL-33
Oligonucleotides		
PFKL-JD-F (5′-3′)	GCGGTCACGTGTAAGGAACA	N/A
PFKL-JD-R	TTCAGAACCAGGAAGAGCCG	N/A
LDHA-JD-F (5′-3′)	CTGTCCCTGGGCTGAATGAC	N/A
LDHA-JD-R	GCATTTCTGCGGCTATGGTG	N/A
MCT1-JD-F (5′-3′)	GCTCGGATCCTTCATTGCTG	N/A
MCT1-JD-R	AGCAACATGGGATCTGAGGT	N/A
SQLE-JD-F (5′-3′)	GGTGTCACCGAAGAAGCCTT	N/A
SQLE-JD-R	GAACCTCCATATGCCGCTGG	N/A

(*Continued on next page*)

Continued

REAGENT or RESOURCE	SOURCE	IDENTIFIER
Software and algorithms		
GraphPad Prism 7	GraphPad	N/A
ImageJ	ImageJ	N/A

RESOURCE AVAILABILITY

Lead contact

Further information and requests for resources and reagents should be directed to and will be fulfilled by the lead contact, Xiaochun Tang at xiaochuntang@jlu.edu.cn.

Materials availability

This study did not generate new unique reagents. All unique reagents generated in this study are available from the lead contact with a completed Material Transfer Agreement.

Data and code availability

- All data reported in this paper will be shared by the lead contact upon request.
- This study did not generate original code.
- Any additional information required to reanalyze the data reported in this paper is available form the lead contact upon request.

EXPERIMENTAL MODEL AND SUBJECT DETAILS

Cell lines

Porcine kidney cell line (PK-15) cells were purchased from ATCC. PK-15 cells were cultured in Dulbecco's modified Eagle's medium supplemented with 5% fetal bovine serum and penicillin-streptomycin. All cells were maintained at 37°C and 5% CO_2. Most culture media were from Gibco unless otherwise noted. Heat-inactivated FBS was purchased from Gibco.

Virus strain

CSFV (Shimen strain) was kindly provided by Dr. Changchun Tu (Academy of Military Medical Sciences, Changchun, China).

METHOD DETAILS

Detection of glucose concentrations

Glucose concentrations were examined by Tissue Cell Glucose Oxidase Assay Kit (Pplygen, China, E1011), according to manufacturer's instructions. The infinite 2000 PRO Microplate Reader (Tecan, Switzerland) was used to measure the absorbance of the samples at 37°C and measured in triplicate.

Detection of lactate concentrations

The lactate concentrations were measured using the lactate assay kit (Nanjing Jiancheng Bioengineering Institute, China, A019-2-1), as directed by the manufacturer. An Infinite 2000 PRO Microplate Reader was used to determine the OD (Tecan, Switzerland). The absorbance of the samples was monitored at 37°C and measured in triplicate. The total protein concentration was used to normalize the data.

Detection of the content of adenosine triphosphate (ATP)

According to the manufacturer's instructions, the content of ATP was detected using an Enhanced ATP Assay Kit (Beyotime, China, S0027). The absorbance of the samples was measured in triplicate at 37°C using an infinite 2000 PRO Microplate Reader (Tecan, Switzerland). The total protein concentration was used to normalize all of the data.

Quantitative real-time PCR (qPCR)

TRNzol-A + Reagent (Tiangen, China, DP424) was used to extract total RNA from PK-15 cells, and the FastKing RT Kit (with gDNase) (Tiangen, China, KR116) was used to reverse transcribe the RNA into cDNA. A BIO-RAD iCycler Thermal Cycler with iQ5 Optical Module for RT-PCR was used to measure fluorescence intensity and amplification plots (Bio-Rad, ABI 7500, iQ5). The primers used in qPCR are listed in Table S1.

Virus one-step growth curve

Infection of PK-15 cells with 200 TCID50 of CSFV (Shimen strain) in a 6-well plate with 80 percent confluence was done in three replicates for each group. The inoculums were replaced with fresh medium one hour after inoculation. At 12, 24, 36, 48, 60, 72, 84, and 96-h post-infection, 200 μL of viral supernatant was harvested, extract viral RNA and reverse transcribe the RNA into cDNA. The viral-genomic copy numbers were detected by qPCR. The virus one-step growth curve was created according to viral-genomic copy numbers.

Transcriptome analysis

PK-15 cells were seeded at a density of 2×10^5 cells per well in 6-well plates to obtain 80–90% confluence before CSFV infection. CSFV (Shimen strain) was infected into PK-15 cells at 200 $TCID_{50}$ and harvested 48 h after infection. TRNzol-A+ reagent was used to isolate total RNA, which was then subjected to RNA deep sequencing and analysis as directed by the manufacturer. The Metascape platform (http://metascape.org/) was used to perform GO and KEGG enrichment pathways (Zhou et al., 2019).

Western blotting (WB)

Western blotting was performed according to the manufacturer's instructions. Equal amounts of proteins were separated on the separating gel using SDS-PAGE, and the protein bands were electrophoretically transferred to PVDF membranes. The ECL-Plus western blotting reagent was used to detect the protein bands. The primary and secondary antibodies involved in the process were shown in Table S2.

Plasmid construction

With the help of online software (http://crispr.mit.edu/), single-guide RNAs (SgRNAs) targeting *PFKL*, *LDHA*, *MCT1*, and *SQLE* were created. The sgRNA oligonucleotides were synthesized (Comate Bioscience, China), annealed, and cloned into the pX330-U6-Chimeric BB-CBh-hSpCas9 empty expression vector (Addgene, 42230) or the pBluescriptSKII + U6-sgRNA(F + E) empty expression vector (Addgene, 74707).

Cell transfection and genotyping of cell clones

Approximately, 3×10^6 PK-15 cells were electrotransfected with 30 μg plasmids in 200 μL of Opti-MEM (GIBCO) using 2-mm gap cuvettes and a BTX ECM 2001 electroporator. The parameters for electrotransfection were as follows: 300 V, 1 ms, 3 pulses for 1 repeat. At 36 h after electrotransfection, cells were plated into five 10-cm dishes at 1.5×10^3 cells per dish. In 48-well plates, single-cell colonies were chosen and cultured. The cell clones were subcultured after reaching 80% confluence, and 20% of each clone was lysed for 1 h at 56°C and 10 min at 95°C in 20 μL of NP40 lysis buffer (0.45 percent NP-40 plus 0.6 percent Proteinase K).

The lysate was used as a PCR template and was subjected to 1% agarose gel electrophoresis. The primers for genotyping are shown in the following table.

Off-target analysis

Cas-OFFinder was used to predict all possible off-target sites (OTSs) for each sgRNA. To identify off-target effects, OTS were analyzed using PCR and DNA sequencing. The primer sequences used for analyzing the off-target activities are listed in Tables S3 and S4.

Detection of extracellular pH (pHe)

The extracellular pH of samples was measured using a high-precision pH meter according to manufacturer's protocol. Samples were monitored at 37°C and measured in triplicate.

Cell viability assays (CCK8 assay)

2×10^3 PK-15 cells were plated in 96-well plates and incubated in 200 μL drug-supplemented medium with 0.1% DMSO or the following drug concentrations standardized to 0.1% DMSO final concentration. Cell viability was measured using a Cell Counting Kit-8 assay (Dojindo, China, CK04) according to the manufacturer's instructions. An infinite 2000 PRO Microplate Reader was used to measure the optical density at 450 nm (OD450 nm) (Tecan, Switzerland). At 37°C, the absorbance of the samples was monitored in triplicate. (Figure S6).

Detection of cholesterol concentrations

A total cholesterol assay kit (Nanjing Jiancheng Bioengineering Institute, China) was used to measure cholesterol levels according to the manufacturer's instructions. With an infinite 2000 PRO Microplate Reader, the cholesterol concentration was measured and calculated using a standard curve (Tecan, Switzerland). At 37°C, the absorbance of the samples was monitored in triplicate. The total protein concentration was used to normalize all of the results.

QUANTIFICATION AND STATISTICAL ANALYSIS

Statistical analysis

All data are expressed as the means ± standard error of the mean (SEM). Statistical differences were determined by unpaired Student's t-test for two-group comparisons and one-way ANOVA with Bonferroni's post-test for multiple group comparisons. All the statistical analyses were completed using the GraphPad Prism 7.0 software.